RESEARCH ON SPECTROSCOPY, OPACITY, AND ATMOSPHERES

NASA Grant NAGW-4272

Annual Report No. 2

For the Period 1 March 1996 through 28 February 1997

Principal Investigator

Dr. Robert L. Kurucz

December 1996

Prepared for
National Aeronautics and Space Administration
Washington, D.C. 20546

Smithsonian Institution
Astrophysical Observatory
Cambridge, MA 02138

> **The Smithsonian** Astrophysical Observatory
> is a member of the
> **Harvard**-Smithsonian Center for Astrophysics

RESEARCH ON SPECTROSCOPY, OPACITY, AND ATMOSPHERES

I spent most of the year moving my office, fighting with administrators, and moving and upgrading my computers. My books, files, and research materials were in a warehouse much of the year.

I made very little progress on atomic and molecular data. I expect to get back into production with the new year. I did upgrade Lyman alpha wing, C I, and Si I opacities in my spectrum sysnthesis program. The changes in Lyman alpha and in Si I produced increased absorption around 160 nm. The C I opacity is increased especially between Lyman alpha and beta. I have been editing NIST data files to use as input into my atomic calculations.

I did not make any new CD-ROMs but continued to distribute the 23 already made. I am setting up a workstation to serve as a Web server so that the model atmospheres, line data, and my publications will be easily available. If I can get funding I will install a CD jukebox.

I did learn a great deal about convection in model atmospheres and the shortcomings of the mixing length formulations for treating it. I corrected a numerical error in my model atmosphere program that occured in the case of weak convection, especially in A and F stars, and I recomputed several thousand convective models. I also investigated the relationship betweeen convective velocity, microturbulent velocity, and opacity that has been ignored up until now. I will produce new grids in the next year to study the effect. It also seems that it is impossible to have both (simple-minded) pulsation and (simple-minded) convection in an atmosphere at the same time because the velocities are comparable. There may be problems with model atmospheres for cepheids. I will continue to investigate.

1996 A new opacity-sampling model atmosphere program for arbitrary
     abundances. In IAU Symposium 176: Stellar Surface Structure,
     K.G. Strassmeier and J.L. Linsky, (Eds.) pp. 523-527.

1996 Rapid calculation of line opacity. To appear in Computational
     Astrophysics, Volume 2, Stellar Physics (ed. R. Kudritzki, D. Mihalas,
     K. Nomoto, and F.-K. Thielemann) Springer-Verlag, Berlin.

1996 Fundamental parameters of Cepheids. IV. Temperature and gravity.
     (D. Bersier, G. Burki, and R.L. Kurucz) submitted to Astronomy and
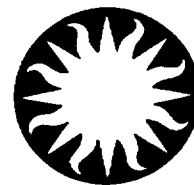   Astrophysics.

1996 Status of the ATLAS12 opacity sampling program and of new programs for
     Rosseland and for distribution function opacity. in 'Model Atmospheres
     and Spectrum Synthesis', eds. S.J. Adelman, F. Kupka and W.W. Weiss,
     A.S.P. Conf. Proc. 108, p. ___.

1996 Model stellar atmospheres and real stellar atmospheres. in 'Model
     Atmospheres and Spectrum Synthesis', eds. S.J. Adelman, F. Kupka and
     W.W. Weiss, A.S.P. Conf. Proc. 108, p. ___.
1996 A calibration of Geneva photometry for B to G stars in terms of Teff,
     log g, and [M/H]. (M, Kuenzli, P. North, R.L. Kurucz, and B. Nicolet)
     submitted to Astronomy and Astrophysics.

Harvard-Smithsonian Center for Astrophysics

MODEL STELLAR ATMOSPHERES
AND
REAL STELLAR ATMOSPHERES

and

STATUS OF THE ATLAS12 OPACITY SAMPLING PROGRAM
AND OF NEW PROGRAMS FOR
ROSSELAND AND FOR DISTRIBUTION FUNCTION OPACITY

Robert L. Kurucz
Harvard-Smithsonian Center for Astrophysics

HARVARD COLLEGE OBSERVATORY   SMITHSONIAN ASTROPHYSICAL OBSERVATORY

60 Garden Street, Cambridge, Massachusetts 02138

MODEL STELLAR ATMOSPHERES
AND
REAL STELLAR ATMOSPHERES

and

STATUS OF THE ATLAS12 OPACITY SAMPLING PROGRAM
AND OF NEW PROGRAMS FOR
ROSSELAND AND FOR DISTRIBUTION FUNCTION OPACITY

Robert L. Kurucz
Harvard-Smithsonian Center for Astrophysics

Model Stellar Atmospheres and Real Stellar Atmospheres

ROBERT L. KURUCZ
Harvard-Smithsonian Center for Astrophysics
60 Garden Street, Cambridge, Massachusetts 02138, USA
e-mail: rkurucz@cfa.harvard.edu

Abstract. I discuss errors in theory and in interpreting observations that are produced by the failure to consider resolution in space, time, and energy. I discuss convection in stellar model atmospheres and in stars. Large errors in abundances are possible such as the factor of ten error in the Li abundance for extreme Population II stars. Finally I discuss the variation of microturbulent velocity with depth, effective temperature, gravity, and abundance. These variations must be dealt with in computing models and grids and in any type of photometric calibration.

1. Introduction

Figure 1 is a photograph taken in a Los Angeles movie theater by Hiroshi Sugimoto. It is an observation. What can we determine about the various resolutions involved? Since fine details are visible in the proscenium, the resolution in x and y must be high. The x-y resolution on the screen must also be high although no details are apparent. Since the picture seems to be in focus everywhere, there are no depth clues about the z resolution. Since it is a black and white photograph, the energy range is the visible and the energy resolution is perhaps 200 nm. The time resolution is one and a half hours. This is a photograph of a whole movie. All of the romance and mystery and tragedy and sex and violence and color have been integrated into a featureless rectangle.

Solar intensity or flux spectrum atlases are produced by integrations over a similar time interval. Stellar spectra that are used to determine the properties of stars and their abundances are also integrations over space and time. How much physics has been integrated away?

2. When is physics valid?

Every observation, measurement, model, and theory has seven characteristic numbers: resolution in space, in time, and in energy, and minimum and maximum energy. Many people never think about these resolutions. A low resolution physics cannot be used to study something in which the physical process of interest occurs at high resolution unless the high resolution effects average out when integrated over the resolution bandpasses. If a theory is

statistical, it cannot be valid if the resolution volume does not contain a large number of particles.

What does the sun, or any convective atmosphere, actually look like? We do not really know yet. There is a very simplified three-dimensional radiation-hydrodynamics calculation discussed in the review by Chan, Nordlund, Steffen, and Stein (1991). It is consistent with the high spatial and temporal resolution observations shown in the review by Topka and Title (1991). We can qualitatively understand the problem by studying Figure 2 taken from Chan et al. This is a plot of the fluid velocity in an x-z plane cut through their three-dimensional box. To quote them exactly: "The ascending flow is broad and diverging; the descending flow is filamentary and converging. The cells span the entire vertical extent of the computational domain. There are no multiple cells in the vertical direction." The rising elements are hot and the falling elements are cold. The filling factor for the cold downward flowing elements is small. The structure changes with time. Nordlund and Dravins (1990) discuss four similar stellar models with many figures. Figure 3 shows the same data as Figure 2 but compressed into one dimension. Figure 4 shows the corresponding T-τ plot. We must remember that every convective model like that in Figure 4 represents a physical reality like that in Figure 2,

There is a solar flux atlas (Kurucz, Furenlid, Brault, and Testerman 1984) that Ingemar Furenlid caused to be produced because he wanted to work with the sun as a star for comparison to other stars. The atlas is pieced together from eight Fourier transform spectrograph scans, each of which was integrated for two hours, so the time resolution is two hours for a given scan. But the scans were made over an eight month period. For studying variability, the resolution can be as bad as eight months. The x and y resolutions are the diameter of the sun. The z resolution (from the formation depths of features in the spectrum) is difficult to estimate. It depends on the signal-to-noise and the number of resolution elements. The first is greater than 3000 and the second is more than one million. It may be possible to find enough weak lines in the wings and shoulders of strong lines to map out relative positions to a few kilometers. Today I think it is to a few tens of kilometers. The resolving power is on the order of 522,000. This is not really good enough for observations made through the atmosphere because it does not resolve the terrestrial lines that must be removed from the spectrum. The sun itself degrades its own flux spectrum by differential rotation and macroturbulent motions. The energy range of the atlas is from 300 to 1300 nm, essentially the range where the sun radiates most of its energy.

To analyze this spectrum, or any other spectrum, we need a theory that works at a similar resolution or better. We use a plane parallel, one-dimensional theoretical or empirical model atmosphere that extends in z through the region where the lines and continuum are formed. The one-dimensional model atmosphere represents the space average of the convective structure over the whole stellar disk (including the center-to-limb variation) and the time average over hours. It is usually possible to compute a model that matches the observed energy distribution around the flux maximum. However, to obtain the match it is necessary to adjust a number of free parameters: effective temperature, surface gravity, microturbulent velocity, and the mixing-length-to-scale-height-ratio in the one-dimensional convective treatment. The microturbulent velocity parameter also produces an adjustment to the line opacity to make up for missing

lines. Since much of the spectrum is produced near the flux maximum, at depths in the atmosphere where the overall flux is produced, averaging should give good results. The parameters of the fitted model may not be those of the star, but the radiation field should be like that of the star. The sun is the only star where the effective temperature and gravity are accurately known. In computing the detailed spectrum, it is possible to adjust the line parameters to match all but the centers of the strongest lines. Since very few lines have atomic data known accurately enough to constrain the model, a match does not necessarily mean that the model is correct.

3. Finding errors

When I first started work as an undergraduate research assistant, I did not know anything about astrophysics or computing. My job was to find all the gf values in the literature, to determine the best data, and to produce a line list for abundance analysis. I was extremely upset to find that the elegant physics I had studied in textbooks was awfully dirty in the real world, and was not necessarily well determined or even true.

The Fe abundance in the sun was too small by a factor of ten because of bad gf values; see Goldberg, Müller, and Aller (1960); Goldberg, Kopp, and Dupree (1964). Between the first and second of these papers, Corliss and Bozman at the National Bureau of Standards measured gf values for 25,000 lines, including 658 for Fe I, and published them in a book (1962). Corliss and Warner (1964) redid the Fe I and measured 2000 lines. Goldberg et al. (1964) used those measurements to find the iron abundance. It came out nearly the same. It is only in the present decade that the error has been reduced below 50%. But it may not be as low as the 10% claimed in modern papers.

This was all extremely educational for me as I tried to understand Fe and all the other elements. I learned not to trust observers, experimentalists, modellers, or theoreticians, and not to trust anything in textbooks or journals. In graduate school I learned to be skeptical of anything that is commonly accepted or taken for granted. I also do not trust what I compute. There can be errors in the programs that are not discovered until some extreme case is considered.

4. Errors introduced by unphysical treatments of convection

There are two fundamental rules of abundance analysis: 1) use weak lines on the linear part of the curve of growth where line strength is directly proportional to abundance, and 2) work with the principal stage of ionization. These rules minimize the effects of errors in the model, in the damping treatment, and in microturbulent velocity. If there is a factor-of-two error in the ionization of a 90% ionized element, the neutral abundance is in error by a factor of two while the ion abundance is in error only by 5%.

Paolo Molaro has complained to me that the Li abundance is sensitive to the convective treatment in my models. Molaro, Bonifacio, and Primas (1995) have computed models with various convective treatments to try to estimate the uncertainty. When Molaro has asked me about it, I have said that mixing-length theory is wrong and that no one is capable of computing real convection. After

the 1994 IAU General Assembly in the Hague, it finally occured to me that if the Li D lines are so sensitive, they must be formed at the top of the convection zone. I looked at a model from my grid (Kurucz 1993) that has the approximate parameters for HD140283, one of the brightest extreme Population II stars: 5750K Teff, 3.5 log g, and [-3.0]. The model is more strongly convective than a solar model because the gravity is lower; the maximum convective velocity is 3.0 km s^{-1} instead of 2.2 in the solar model. The higher convective velocity implies higher microturbulent and macroturbulent velocities as well. It also has a much flatter temperature gradient than the sun as shown in Figure 5 because the low abundance produces little backwarming and so little surface cooling. The model is plotted in Figure 6 with the Schwarzschild-criterion top-of-the-convection-zone and the depth of formation of the D lines marked. Li is more than 99.94% ionized at that depth. The chance that the Li abundance can be found by using a one-dimensional model atmosphere is therefore essentially zero. It can be determined only by doing a real three-dimensional radiation-hydrodynamics convection calculation that is considerably beyond the state-of-the-art because of the complexity of treating the radiative transfer realistically.

I have never paid much attention to the measurement of the Li abundance. I assumed that it was a straightforward problem and that the Population II observers were treating it correctly. I have computed the Li D line region in the sun as part of computing the whole spectrum to test my line data as shown in Figure 7. Few people realize that in the sun one half the lines are still not identified. In Figure 7 there are large numbers of lines in the spectrum stronger than the Li lines that are completely missing from the line list. The nineteen components of the D lines and the other lines are listed in Kurucz (1995). Most of the lines are CN. In extreme Population II stars where the Li abundance is higher than in the sun and the metal abundance is much lower, the missing lines do not matter. They may matter in Population I stars.

The mixing-length theory itself produces a temperature bifurcation that is assumed to average out in the physics. I have an old model atmosphere program, ATLAS11, that is useless except for demonstrating this bifurcation. It uses a two-stream mixing-length formulation in which half the area of the star is a hot upward stream and the other half is a cold downward stream. Figure 8 shows the temperature bifurcation that program produces from the mean model. There can be 3000K temperature differences, but they are constrained to the convection zone.

The more realistic three-dimensional calculations show that hot and cold streams continue toward the surface and also that the hot streams are 80 or 90% of the area. I decided that a better approximation was to consider self-consistent single-component models with a range of effective temperatures. In Figure 9 I plot the mean 5750,3.5,[−3] model and its siblings within 1000K. It shows a temperature range qualitatively similar to that shown for a three-dimensional model in Figure 19c in Nordlund and Dravins (1990). Also plotted for each model is the log fraction of neutral lithium over total lithium. The neutral fraction is determined mainly by the electron number density which increases by six orders of magnitude from top to bottom of the atmosphere.

For each of the nine models I did a complete non-LTE calculation for Li including all levels and lines up through n = 9. I computed the equivalent width of the D lines, assuming no ^{6}Li, both for Li abundance 2.08 and 3 as listed in Kurucz (1995). The non-LTE effect was never more than a few percent in

accordance with Carlsson, Rutten, Bruls, and Shchukina (1994). In retrospect, the whole calculation could have been done in LTE with the same results. The mean model has approximately the observed equivalent width for HD140283. So does the model 1000K hotter with high abundance. The cold model has a six times larger equivalent width for the high abundance and it also has a wide rectangular profile. The profiles are plotted in Figure 10. A two-component model with 80 to 90% of the surface hot and the remainder cold would produce the wrong equivalent width. It would also produce a bimodal line with a shallow rectangular base and a triangular center, unlike the purely triangular profile actually observed (Hobbs and Thorburn 1994). The observed profile is similar to the triangular profiles in Figure 10 and shows that less than roughly 3%, and perhaps none, of the observed space-time volume has strong Li D lines. Figure 11 shows the mean intensity in the Balmer continuum for the hot and cold models at the depth of formation of the D lines in the mean model. The ^{2}S continuum starts at 230 nm. The ^{2}P continuum starts at 350 nm. The mean intensity is between one and two orders of magnitude greater in the hot component. Figure 11 also shows the total opacity at the same point. The cold component is fifteen times more transparent because it has a much lower H(n=2) population. The cold components cannot be optically thick to the ionizing radiation from the hot component. Therefore, Li is over-ionized in the cold component. In a real convective calculation, the cool component is filamentary and the transfer is computed in all directions. The final result will be that the real star with ten times as much Li produces the same equivalent width as that produced by a one-dimensional model with Li abundance 2.08 .

Elements other than Li may be affected as well. At the same depth as for Li, Ca is 99.9% ionized; Na 99.5%; Fe 97.8%. The metallicity may be determined incorrectly. Be and B may be safe, 78.5% and 69.8%. The hydrides and CO are probably very sensitive.

Problems like this can arise in any convective atmosphere for any species that does not average in space and time to the one-dimensional model predictions. In the sun this may account for the remaining uncertainties with Fe I found by Blackwell, Lynas-Gray, and Smith (1995) and for the cool CO fundamental line cores (Ayres and Testerman 1981). Problems with K giant abundances may also arise from similar mechanisms. Because of the hot and cold components, the ultraviolet photospheric flux in any convective star must be higher than a one-dimensional model predicts (Bikmaev 1994). Then, by flux conservation, the flux redward of the flux maximum must be lower. It is fit by a model with lower effective temperature than that of the star. This flux "distortion" may be responsible for Short and Lester's (1994) problems with the ultraviolet flux of Arcturus.

The following qualitative predictions result from the exponential falloff of the flux blueward of the flux maximum:

1) the Balmer continuum in all convective stars is higher than predicted by a one-dimensional model;

2) in G stars, including the sun, the discrepancy reaches up to about 400nm;

3) in K stars it reaches to about 500nm;

4) in M stars the whole Paschen continuum is higher;

5) flux from a temperature minimum and a chromospheric temperature rise masks this photospheric effect at short wavelengths, but the increased mean intensity still affects photoionization rates in photospheric non-LTE calculations;

6) the spectrum predicted from a one-dimensional model for the exponential falloff region, and abundances derived therefrom, are systematically in error;

7) limb-darkening predicted from a one-dimensional model for the exponential falloff region is systematically in error.

In addition, the strong Boltzmann temperature dependence of the second level of hydrogen implies that the Balmer line wings are preferentially formed in the hotter convective elements. A single-component model that matches Balmer line wings has a higher effective temperature than the star.

5. Variation of convection in a model atmosphere grid

The first point to emphasize is that no matter how convection is computed in one dimension, it is wrong. The arguments among stellar atmospheres researchers about one dimensional models are not about wrong or right but about different kinds of wrongness. There is no Schwarzschild criterion in a convective atmosphere. The derivatives are not defined in convecting elements. There is no overshooting in the atmosphere because there is nothing to overshoot. Convection does not stop where the models pretend it does. The top of the convection zone extends up to log $\tau_{Ross} = -3$ or -4 where the real radial velocity of the elements goes to zero. When convection is weak, it is not in thin layers, it is in separated (in space and time) plumes that do not turn over but dissipate. Only when the number of plumes becomes large enough for the tops to collide does matter begin to flow downward.

I finally started plotting the fraction of convective flux and the convective velocity on the T-log τ_{Ross} plots for the model atmospheres so that I could try to understand their behavior. There appear to be three types of convection in the atmosphere as shown in Figures 12–14. In normal convection, Figure 12, the convective fraction increases toward the bottom of the atmosphere. In real stars the atmospheric convection connects with the envelope convection. The convective velocity increases rapidly downward, reaches a maximum, and flattens out. The abundances in the atmosphere must be the same as those in the envelope immediately below the atmosphere because of mixing. In the second and third types of model-atmosphere convection, the convection zone is wholly contained in the atmosphere in a thin layer. The convective fraction and the convective velocity are thin spikes. There is no connection to any convection beneath the atmosphere. The abundances in the atmosphere are decoupled from those in the envelope beneath the atmosphere. I do not know if this is also true in real stars. In the second type, Figure 13, the convective flux is significant. In the third type, Figure 14, the convective flux is so small that it may be artifactual. The real star may actually be in radiative equilibrium, or the convection may occur only in plumes. In plume convection the plumes occupy only a small space-time fraction of the atmosphere. Hot elements rise through the atmosphere and dissipate. The star appears to have warm spots like rubeola. There is no small scale downward motion. Obviously mixing-length convection has even less to do with plume convection than with normal convection. The convective velocities predicted by the model atmospheres programs are meaningless. There may be interesting effects in real giant and supergiant stars if the plume velocities reach sound speed. It is only when the plumes become so numerous that the

flaring tops collide and condense that downward moving filaments are formed and "normal" convection begins.

Figures 15 and 16 show all my solar abundance convective models with microturbulent velocity 2 km s^{-1}. Figure 15 plots the maximum convective fraction. It rises from 90 to 97 percent as the effective temperature increases and then suddenly drops as the convection retreats into the atmosphere. The log g = 5 models can be strongy convective up to 8000K. The lowest gravity models are strongly convective only up to 5500K. Figure 16 show the maximum convective velocity. The velocity rises smoothly to a peak at the maximum convection and then drops rapidly. The variation with microturbulent velocity is minimal. The variation with abundance is small. For example, the maximum convective velocities for the 6000,4 models are 2.6, 2.6, 2.6, 2.7, 2.7, 2.8, 2.9, 3.0, 3.1 km s^{-1} for abundances [−3.0] to [+1.0] by 0.5. Solar is 2.9 km s^{-1}.

6. Microturbulent velocity

Microturbulent velocity is a parameter that is generally not considered physically except in the sun. Usually it is treated as the parameter that minimizes scatter among lines of the same ion in abundance analyses. Figure 17 shows the temperature versus optical depth for the empirical solar Model C of Fontenla, Avrett, and Loeser (1993). It also shows the empirical (central intensity) microturbulent velocity versus optical depth determined from line profiles. I have schematically divided it into microturbulent velocity that is produced by convective motions that must go to zero at or below the temperature minimum, and into microturbulent velocity that is produced by the waves that heat the chromosphere. I suggest that all "normally" convective stars have behavior like this. This microturbulent velocity is not the microturbulent velocity found in equivalent width abundance analyses. In the sun an equivalent width determination of microturbulent velocity from the flux spectrum yields Vturb < 1 km s^{-1}. It is also not the Vturb of line opacity tables. My solar model has Vturb = 1.5 km s^{-1} in order to make up for missing lines that have not yet been included in the line list. We know for certain that the microturbulent velocity varies with depth, that the opacity is strongly dependent on microturbulent velocity, and that the model atmospheres do not include depth-dependent microturbulent velocity. We also know that stars have chromospheres and temperature minima and that the radiative-convective equilibrium models do not have a temperature minimum or a chromosphere. I suggest a number of ad hoc experiments. In Figure 18 I have weighted the maximum convective velocity by the maximum convective fraction. I treat this weighted velocity Vbot as the microturbulent velocity at the bottom of the atmosphere. It agrees with the empirical value in the sun. Then I take the depth dependence of the microturbulent velocity produced by convection in the sun and I scale to Vbot. Figure 18 then gives the variation of microturbulent velocity with temperature and gravity as long as we stay on the cool side of the maximum. And, since we do not understand what is happening on the hot side, let us blindly do the same there. One thing we know for certain is that there can be no microturbulent velocity produced by convection if there is no convection. ATLAS9 can treat Vturb as as a variable and can interpolate in the distribution function tables for Vturb from 0 to 8 km s^{-1}. I plan to compute some sample models to see how

this works out even though it is horribly inelegant. One can also guess that the "mean" microturbulent velocity must be on the order of one half Vbot. Vbot/2 should correspond to the number found from equivalent widths. It would be the number for pretabulated line opacity if there were no missing lines.

If having Vturb = 0 at the top of a model is unappealing, it can be set to a minimum Vturb = max(Vturb, 0.28 Vbot) as in the sun. If you want to see where the chromosphere starts to affect the spectrum, take a converged model and change the temperatures to max(T, 0.76 Teff) as in the sun, and compute the flux both ways. There will be a point in the visible or ultraviolet where the two fluxes diverge.

Microturbulent velocity varies with effective temperature and gravity and abundance. When comparing the properties of two stars, the change in microturbulent velocity must be accounted for. When a pulsating star changes effective temperature and gravity, it is also changing microturbulent velocity. When comparing two phases, the change in microturbulent velocity must be accounted for. If two stars have the same effective temperature and gravity, the one with the higher abundances will have higher microturbulent velocity.

7. Conclusion

Convective model atmospheres must be used with caution when the properties predicted by the model, such as those listed in Section 4, may not represent the space-time average of the real properties of stars.

It is surprising that we can make any sense at all of convective stars. Apparently, many of the physical complications really do average out most of the time, or perhaps the errors cancel most of the time, or perhaps we delude ourselves most of the time.

References

Ayres, T.R. and Testerman, L. 1981, ApJ 245, 1124-1140.

Bikmaev, I. 1994, personal communication.

Blackwell, D.E., Lynas-Gray, A.E., and Smith, G. 1995, A&A, 296, 217.

Carlsson, M., Rutten, R.J., Bruls, J.H.M.J., and Shchukina, N.G. 1994, A&A, 288, 860.

Chan, K.L., Nordlund, Å, Steffen, M., Stein, R.F. 1991, *Solar Interior and Atmosphere* (Tucson: U. of Arizona Press) 223-274.

Corliss, C.H. and Bozman, W.R. 1962, *Experimental Transition Probabilities for Spectral Lines of Seventy Atoms*, NBS Monograph 53.

Corliss, C.H. and Warner, B. 1964, ApJSupp 8, 395..

Fontenla, J.M., Avrett, E.H., and Loeser, R. 1993. ApJ 406, 319-345.

Goldberg, L., Kopp, R.A., and Dupree, A.K. 1964, ApJ, 140, 707.

Goldberg, L., Müller, E., and Aller, L.H. 1960, ApJSupp 5, 1.

Hobbs, L.M. and Thorburn, J. 1994, ApJ, 428, L25.

Kurucz, R.L. 1993, ATLAS9 Stellar Atmosphere Programs and 2 km/s grid. Kurucz CD-ROM No. 13.

Kurucz, R.L, Furenlid, I., Brault, J., and Testerman, L. 1984, Solar Flux Atlas from 296 to 1300 nm, (Sunspot, N.M.: National Solar Observatory)

Molaro, P., Bonifacio, P., and Primas, F. 1995 in 22nd IAU General Assembly Joint Discussion 11, Stellar and Interstellar Lithium and Primordial Nucleosynthesis, Mem. Soc. Astron. Ital. 66, 323-332.

Nordlund, Å. and Dravins, D. 1990, A&A 228, 155.

Short, C.I. and Lester, J.B. 1994, ApJ 436, L365.

Topka, K.P. and Title, A.M. 1991, *Solar Interior and Atmosphere* (Tucson: U. of Arizona Press) 727-747.

FIGURE CAPTIONS

Figure 1. The photograph *Metropolitan Orpheum, Los Angeles*, 1993 by Hiroshi Sugimoto. Used by permission of Sonnabend Gallery, New York. Print courtesy of Fogg Art Museum, Harvard University.

Figure 2. A simplified three-dimensional radiation-hydrodynamics calculation discussed in the review by Chan, Nordlund, Steffen, and Stein (1991). This is a plot of the fluid velocity in an x-z plane cut through their three-dimensional box. To quote them exactly: "The ascending flow is broad and diverging; the descending flow is filamentary and converging. The cells span the entire vertical extent of the computational domain. There are no multiple cells in the vertical direction." The rising elements are hot and the falling elements are cold. The filling factor for the cold downward flowing elements is small. The structure changes with time.

Figure 3. The same as Figure 2 but compressed into one dimension.

Figure 4. The solar model from Kurucz grid (1993) that corresponds to the line in Figure 3. Every convective model like this one represents a physical reality like that in Figure 2.

Figure 5. A model from Kurucz grid (1993) that has the approximate parameters for HD140283: 5750K Teff, 3.5 log g, and [-3.0] log metal abundance relative to solar. It is plotted together with the solar model of the same grid. Because of the low line opacity it has less backwarming and less surface cooling than the solar model.

Figure 6. A model from Kurucz grid (1993) that has the approximate parameters for HD140283: 5750K Teff, 3.5 log g, and [-3.0] log metal abundance relative to solar. The Schwarzschild-criterion top-of-the-convection-zone and the depth of formation of the D lines are indicated.

Figure 7. The computed Li D line region in the sun. Complete line listings are given in Tables 1 and 2 of Kurucz (1993). The stronger lines are labelled here. The first number in each label is the last three digits of the wavelength. The second field is the identification, i.e. $3.00 = $ Li I, $607\ 12 = {}^{12}C^{14}N$. The third field is the lower energy level in cm^{-1}. The fource field is the per mil residual intensity at line center if the line were computed in isolation. The signed numbers are wavelength or log gf adjustments described in Table 2 of Kurucz (1995).

Figure 8. The temperature bifurcation produced by the ATLAS11 program for the mean model shown in Figure 2. ATLAS11 uses a two-stream mixing-length formulation in which half the area of the star is a hot upward stream and the other half is a cold downward stream.

Figure 9. The mean model and its siblings within 1000K from the Kurucz grid (1993). The log fraction of neutral Li is also plotted.

Figure 10. Non-LTE Li D residual flux profiles computed for the hot, cold, and mean models. The mean model with a standard Li abundance has approximately the observed equivalent width for HD140283. So does the model 1000K hotter with high Li abundance. The cold model has a six times larger equivalent width for the high abundance and it also has a wide rectangular profile.

Figure 11. The mean intensity J_ν in ergs $cm^{-2}s^{-1}ster^{-1}$ and total opacity κ_ν in cm^2g^{-1} in the Balmer continuum for the hot and cold models at the depth of formation of the D lines in the mean model. The Li ^{2}S continuum starts at 230 nm. The Li ^{2}P continuum starts at 350 nm. The mean intensity is between one and two orders of magnitude greater in the hot component. The cold component is about fifteen times more transparent.

Figure 12. The same solar model as in Figure 4 with fraction of convective flux and convective velocity in km s^{-1}.

Figure 13. A model from the Kurucz (1993) grid with the convective zone completely contained within the atmosphere.

Figure 14. A model from the Kurucz (1993) grid with the convective zone completely contained within the atmosphere and a very small convective fraction.

Figure 15. The maximum convective fraction for a whole grid of convective models (Kurucz 1993).

Figure 16. The maximum convective velocity for a whole grid of convective models (Kurucz 1993).

Figure 17. The empirical solar Model C of Fontenla, Avrett, and Loeser (1993) showing both the temperature and the microturbulent velocity variation with Rosseland optical depth.

Figure 18. The maximum convective velocity weighted by the maximum convective fraction for a whole grid of convective models (Kurucz 1993). This may be an ad hoc estimator of the microturbulent velocity at the bottom of the atmosphere.
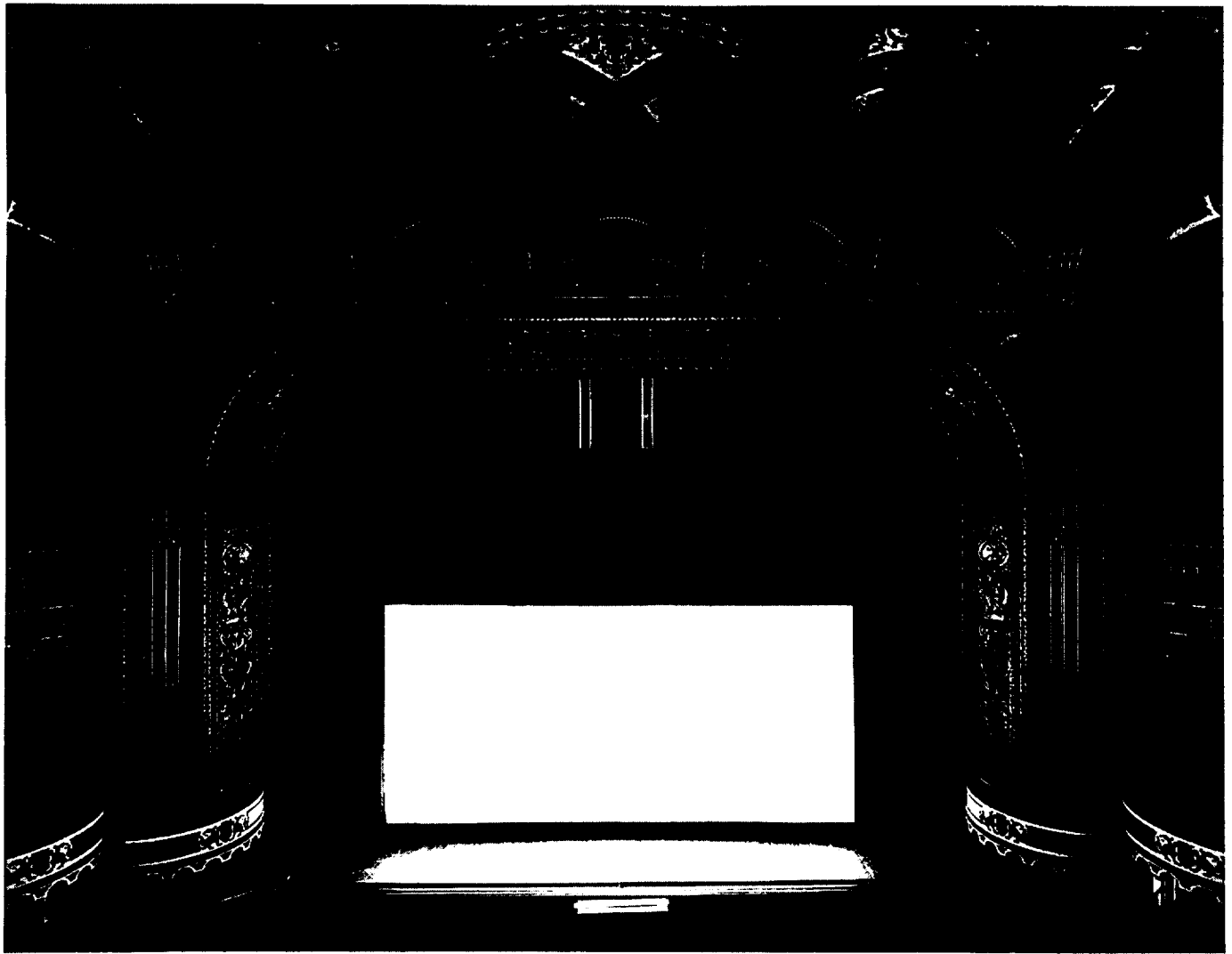
Figure 1. The photograph *Metropolitan Orpheum, Los Angeles, 1993* by Hiroshi Sugimoto. Used by permission of Sonnabend Gallery, New York. Print courtesy of Fogg Art Museum, Harvard University.
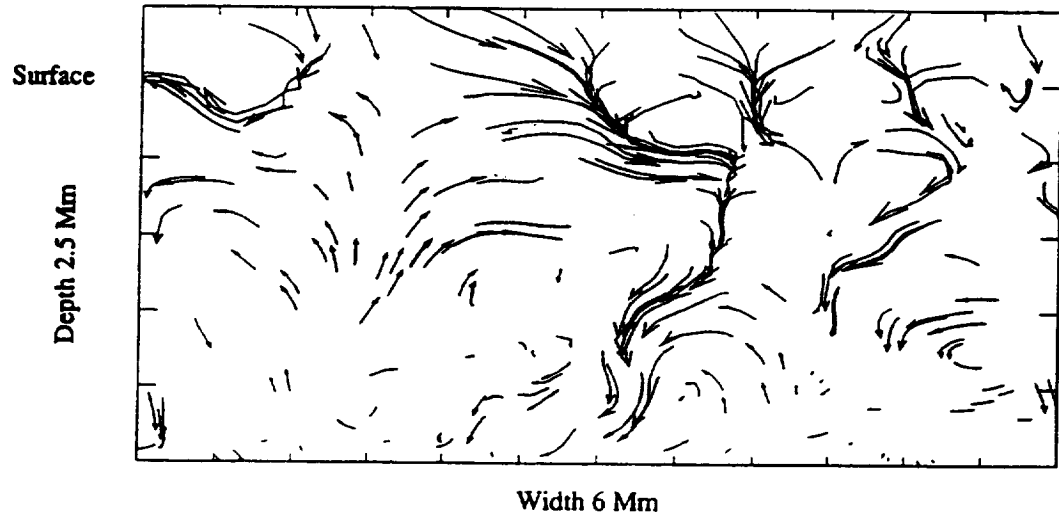
Figure 2. A simplified three-dimensional radiation-hydrodynamics calculation discussed in the review by Chan, Nordlund, Steffen, and Stein (1991). This is a plot of the fluid velocity in an x-z plane cut through their three-dimensional box. To quote them exactly: "The ascending flow is broad and diverging; the descending flow is filamentary and converging. The cells span the entire vertical extent of the computational domain. There are no multiple cells in the vertical direction." The rising elements are hot and the falling elements are cold. The filling factor for the cold downward flowing elements is small. The structure changes with time.

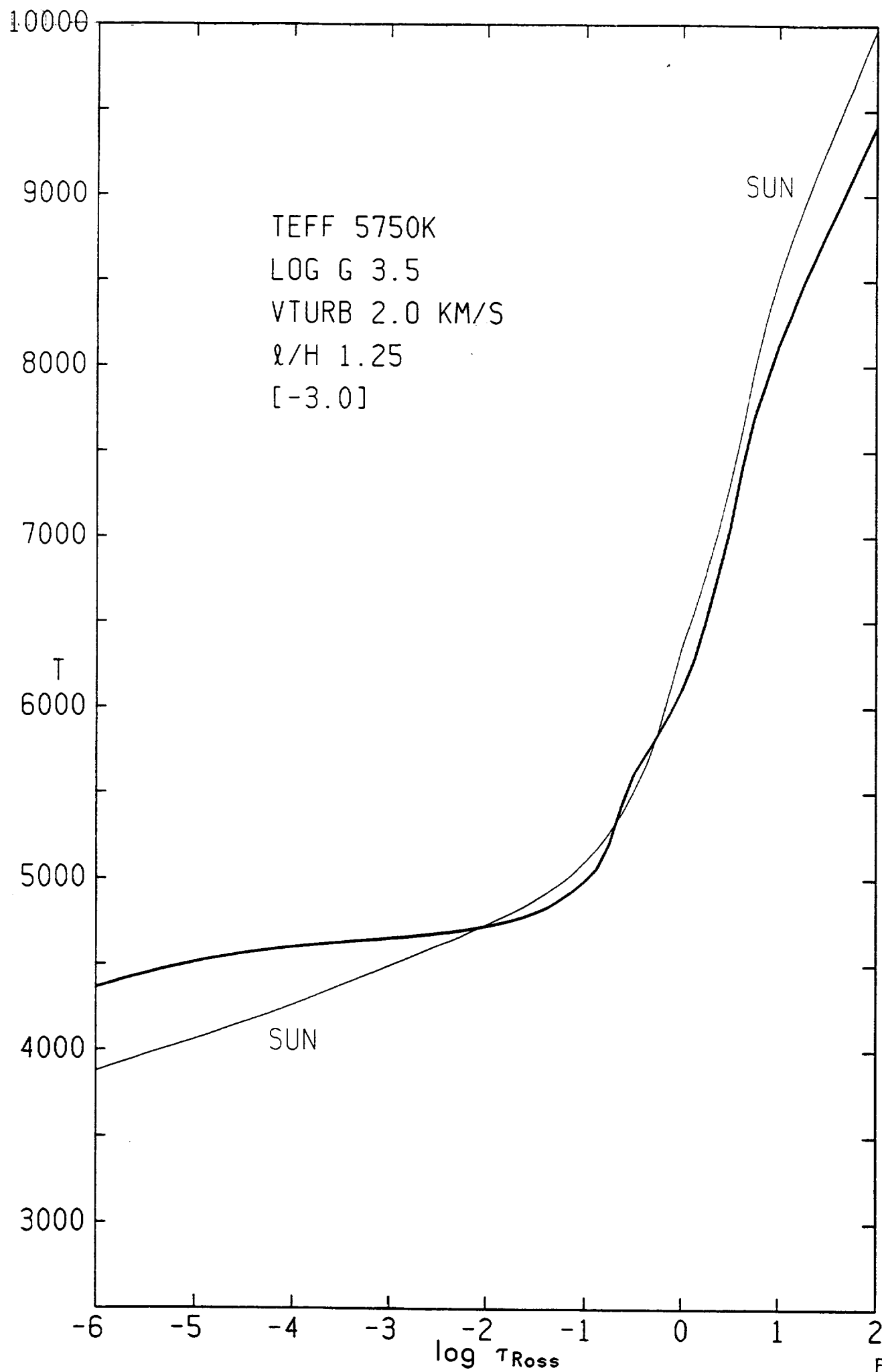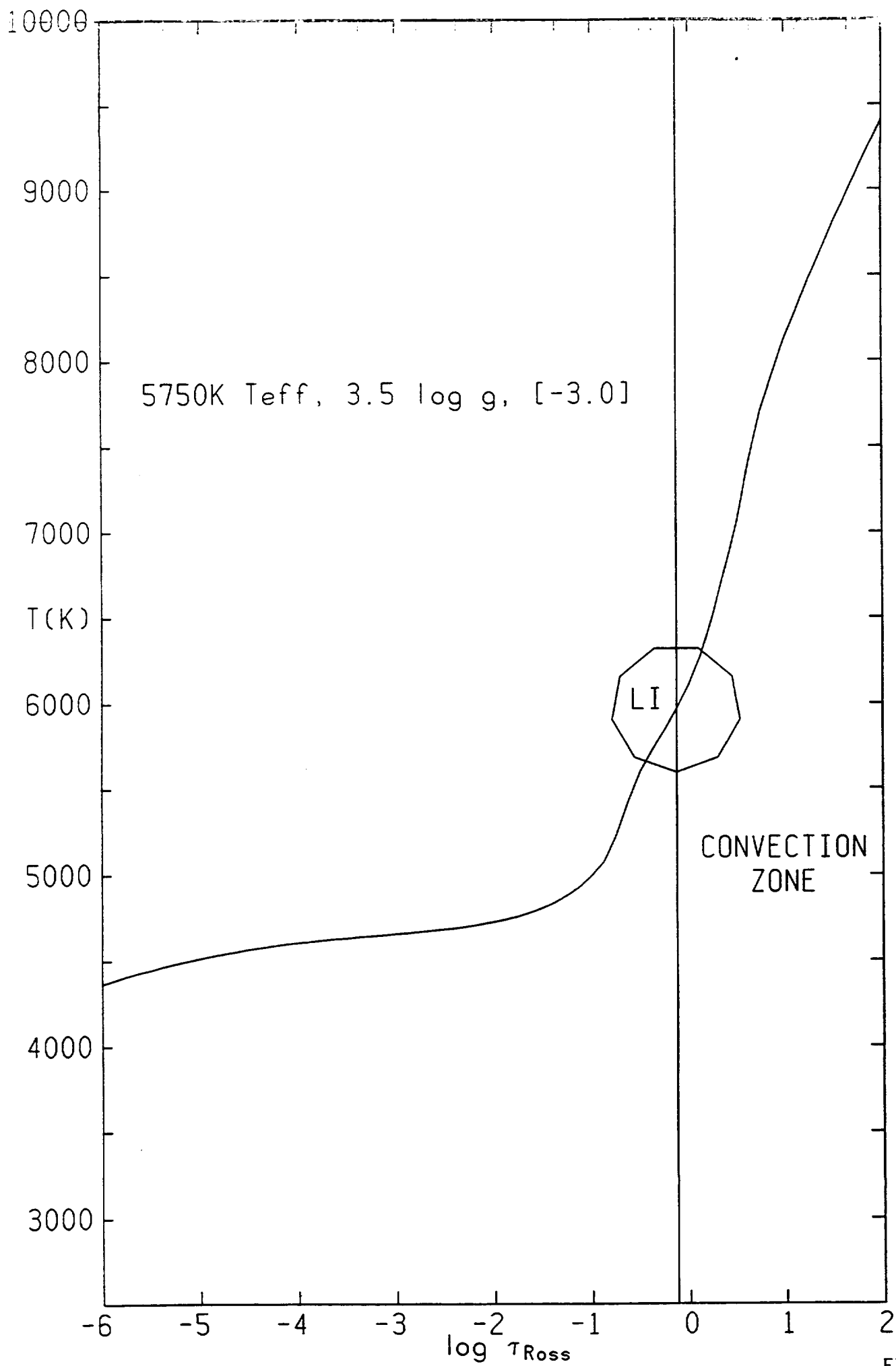Figure 3. The same as Figure 2 but compressed into one dimension.

SUN
TEFF 5777K
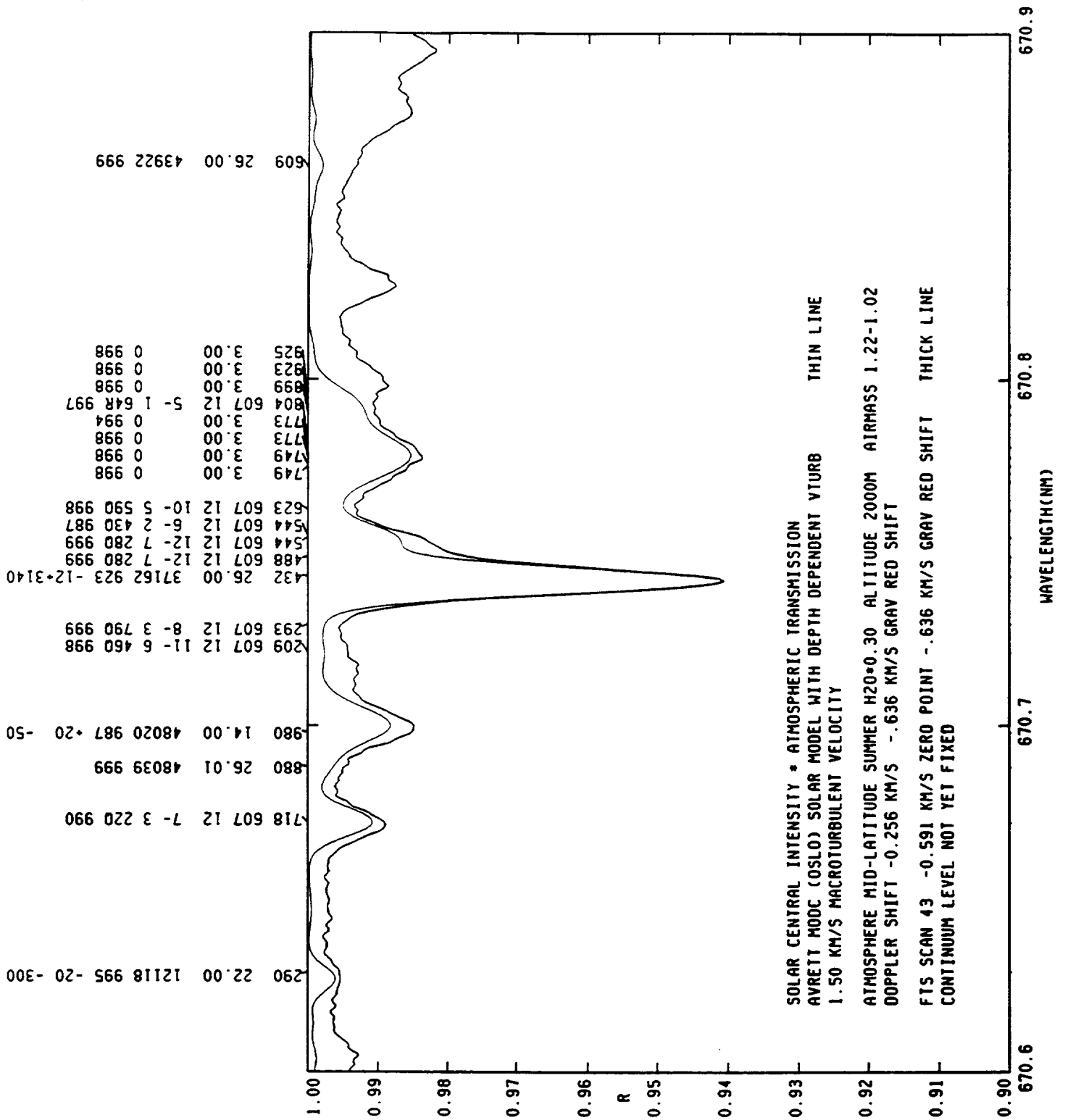LOG G 4.4377
VTURB 1.5 KM/S
ℓ/H 1.25

FIG. 4

FIG. 5

5750K Teff, 3.5 log g, [-3.0]

LI

CONVECTION ZONE

T(K)

log τ_{Ross}

FIG. 6

FIG. 7

TWO-STREAM CONVECTION
5750K Teff, 3.5 log g, [-3.0]

HOT

COOL

LI

CONVECTION
ZONE

T(K)

log τ_{Ross}

FIG. 8

FIG. 9

FIG. 10

FIG. 11

FIG. 12

TEFF 7000K
LOG G 2.0
VTURB 2.0 KM/S
ℓ/H 1.25

VCONV

T

T

CONVECTIVE FRACTION

FIG. 13

TEFF 7000K
LOG G 1.0
VTURB 2.0 KM/S
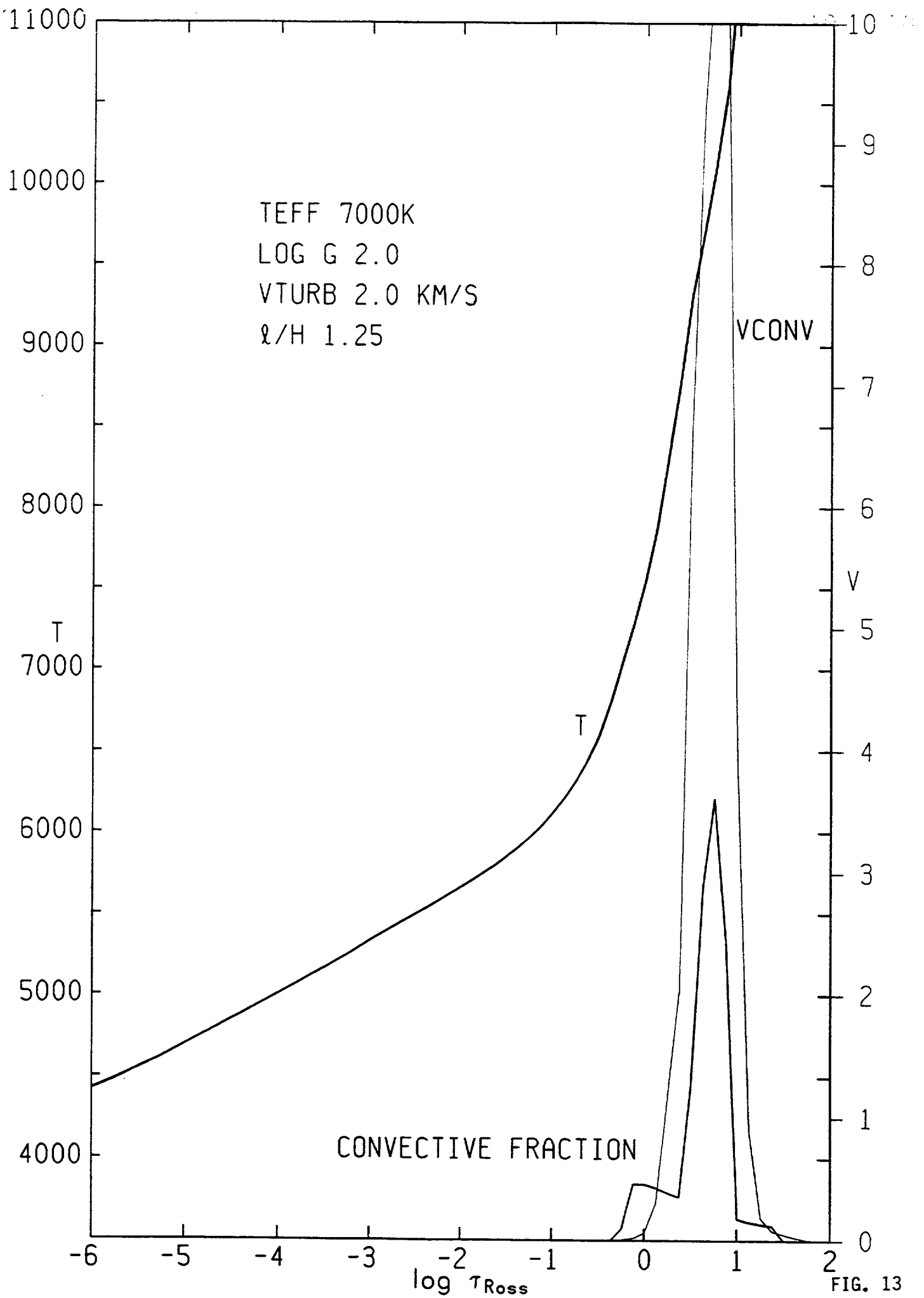ℓ/H 1.25

T

VCONV

CONVECTIVE FRACTION

FIG. 14

LOG G 0.0
0.5
1.0
1.5
2.0
2.5
3.0
3.5
4.0 5.0
4.5

CONVECTIVE MODELS
[0.0] 2 KM/S
MAX CONVECTIVE
FRACTION

$\frac{F_{CONV}}{F_{TOT}}$

TEFF

FIG. 15

CONVECTIVE MODELS
[0.0] 2 KM/S
MAX CONVECTIVE VELOCITY

FIG. 16

EMPIRICAL SOLAR MODEL C
EMPIRICAL MICROTURBULENT VELOCITY

VTURB FROM WAVES

TOTAL VTURB

VTURB FROM CONVECTION

$\log \tau_{Ross}$

FIG. 17

CONVECTIVE MODELS [0.0] 2 KM/S
MAX CONVECTIVE VELOCITY ×
MAX CONVECTIVE FRACTION
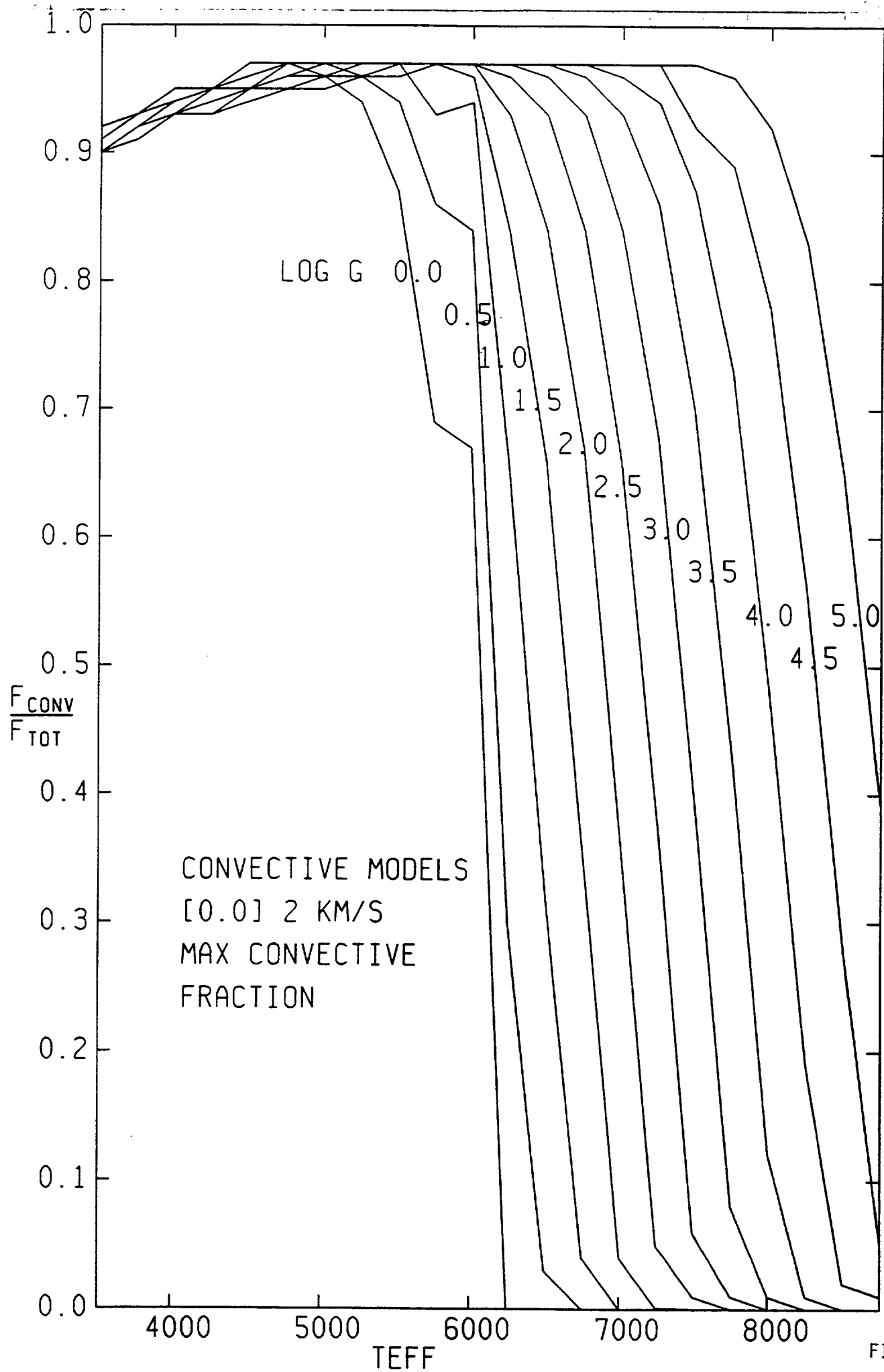
LOG G 0.0

0.5

1.0

1.5

2.0

2.5

3.0

3.5

4.0

4.5

5.0

VCONV

TEFF
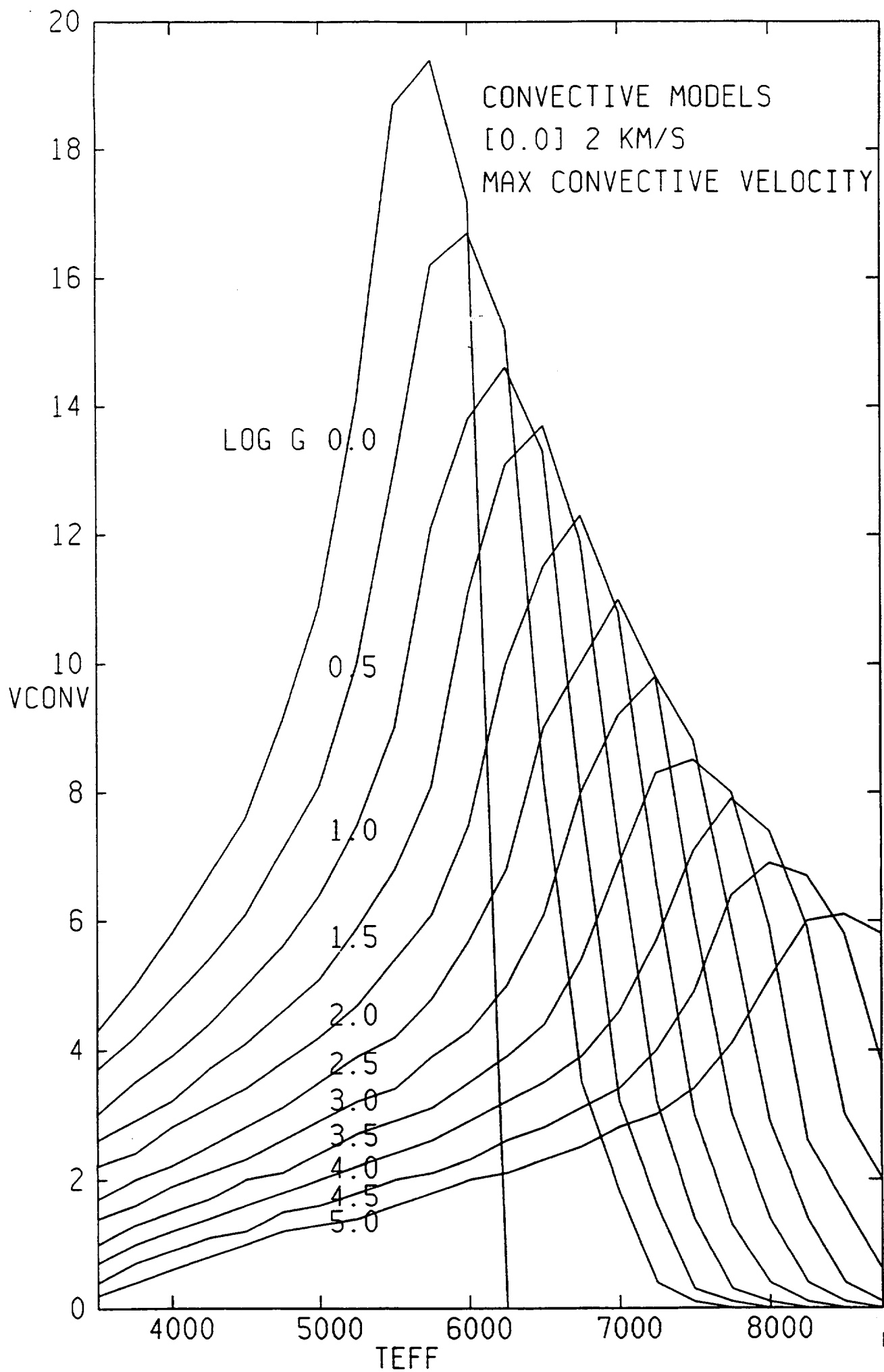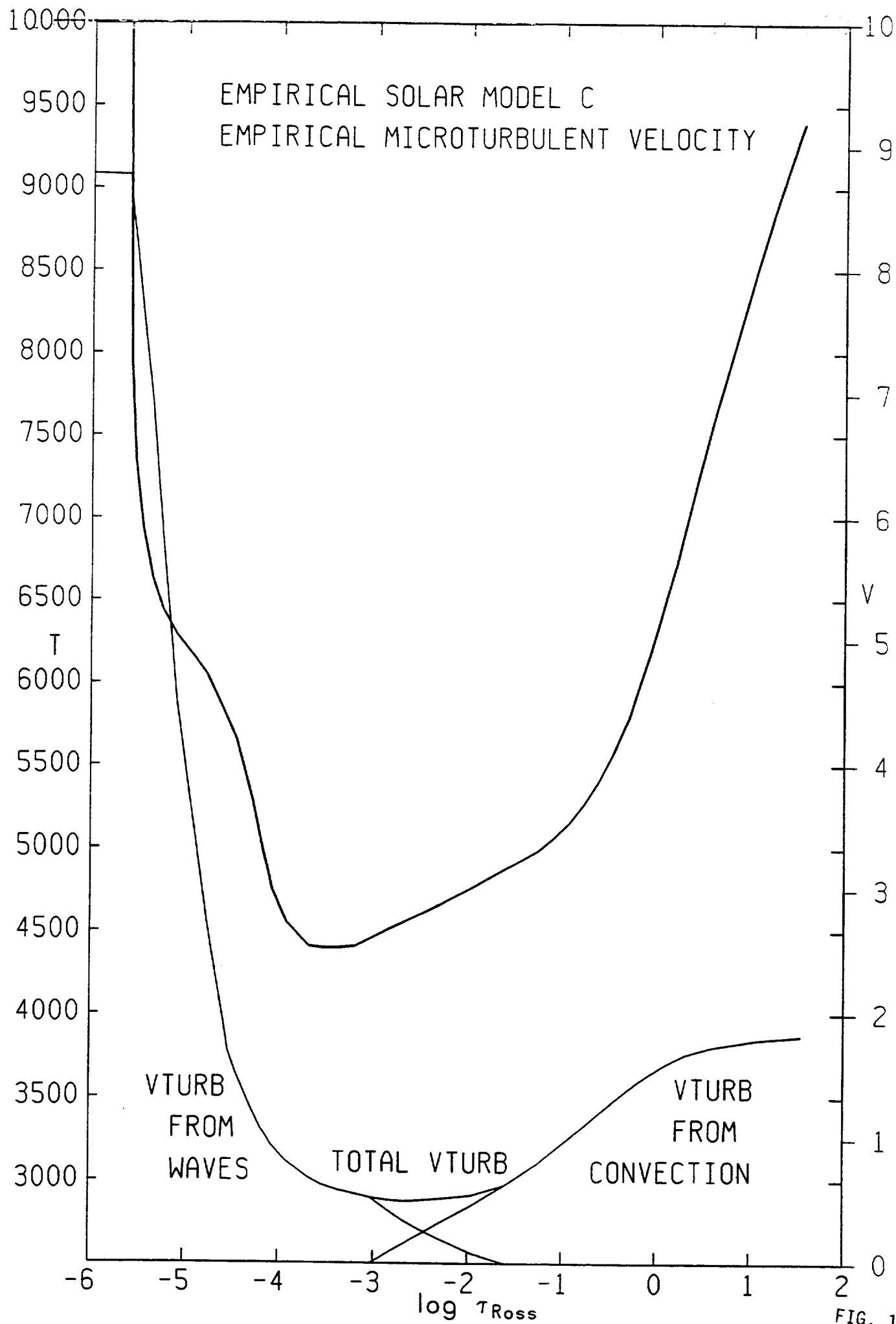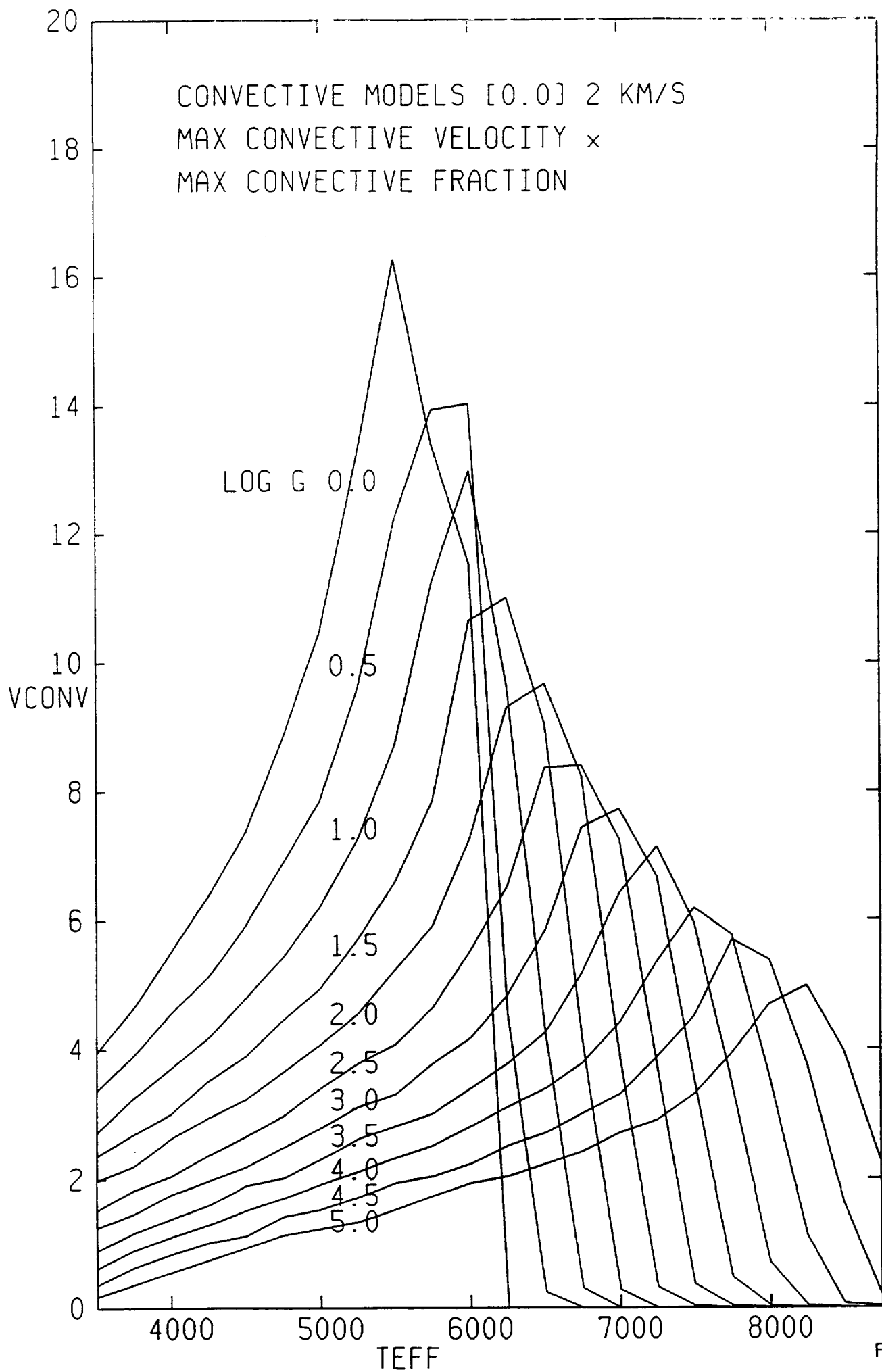
FIG. 18

Status of the ATLAS12 Opacity Sampling Program and of New Programs for Rosseland and for Distribution Function Opacity

ROBERT L. KURUCZ

Harvard-Smithsonian Center for Astrophysics

60 Garden Street, Cambridge, Massachusetts 02138, USA

e-mail: rkurucz@cfa.harvard.edu

Abstract.   I have developed a new opacity-sampling version of my model atmosphere program called ATLAS12. It recognizes more than 1000 atomic and molecular species, each in up to 10 isotopic forms. It can treat all ions of the elements up through Zn and the first 5 ions of heavier elements up through Es. The elemental and isotopic abundances are treated as variables with depth. At present ATLAS12 reads atomic line data from Kurucz CD-ROM 1 and diatomic molecular data from Kurucz CD-ROM 15. For each line the wavelength, identification, lower energy level, gf, radiative, Stark, and van der Waals damping constants are packed into 16 bytes. At each wavelength point in a frequency integration the Voigt profiles of all the significant nearby lines are computed and summed. The H, He, and auto-ionizing lines are treated with the appropriate profile functions.

The fluxes predicted by ATLAS12 are not accurate in intermediate or narrow bandpass intervals because the sample size is too small. A special stripped version of the spectrum synthesis program SYNTHE is used to generate the surface flux for the converged model using the line data on CD-ROMs 1 and 15. That high resolution spectrum can be used directly or can be instrumentally broadened to compare to low resolution observations. Versions of SYNTHE are being developed for computing Rosseland opacity and for computing total or line distribution function opacity.

ATLAS12 can be used to produce improved models for Am and Ap stars. It should be very useful for investigating diffusion effects in atmospheres. It can be used to model exciting stars for H II regions with abundances consistent with those of the H II region. These programs and line files will be distributed on CD-ROMs.

1. Introduction

There are three methods for dealing with line opacity in a model stellar atmosphere. The first is direct calculation of the spectrum of all the lines which can number more than 100 million. It requires a wavelength resolution small enough to resolve the spectrum, smaller than the Doppler width. In an A star

model a resolving power of 500000 produces 3.5 million points. Iterating such a model to convergence is just beyond the state of the art.

The second method is to sample the spectrum by choosing a small number of wavelength points that do not resolve the spectrum in detail. In computing a model the quantity of interest is the integral over the spectrum at each depth which determines the total energy flowing through the atmosphere. Only 1% as many points as are used in the detailed calculation are needed to get accurate integrals. This approach is called opacity sampling.

The third approach is to tabulate statistical distribution functions for the line opacity as a function of temperature and pressure for a fixed set of abundances. The complete opacity spectrum is computed for each temperature-pressure pair and then divided into small wavelength intervals. For each interval a distribution function is computed that tells the fraction of the interval having opacity less than a given value. I have performed distribution function calculations for many scaled solar abundances and I have distributed the tables on Kurucz CD-ROMs 2 to 12. By using these tables a model can be computed for the given abundances using only a few hundred wavelength points. A large amount of computer time is required in the pretabulation but the models can be computed quickly and in large grids.

ATLAS12 is an opacity sampling program that I originally wrote in 1992 to allow computation of models with individual abundances. It is described in Kurucz (1993). The reader should consult that paper for details about ATLAS12 and about my existing grids of models computed with scaled solar abundance distribution function line opacities. That paper has figures showing sample calculations. Castelli and Kurucz (1994) present an ATLAS12 model for Vega.

ATLAS12 seemed to be working well and had no trouble producing models for A stars with abundances within a factor of three of solar. Fiorella Castelli and I were able to compute models for Vega and Sirius including variations in helium abundance. However when I subsequently tried to compute models that were 50% helium, the program would no longer converge. I tried various schemes such as computing a series of models with helium abundance gradually increasing from solar. Nothing worked. I finally understood that the program uses pretabulated Rosseland opacity in two places, in the temperature correction to account for the change in optical depth as the temperature changes, and in convection to determine the opacities of hot and cold elements. If the Rosseland table was not far off, as in the case of Vega and Sirius, the program would work because iteration made up for the small errors. But with large opacity changes, it was hopeless. The pretabulated Rosseland opacity was an end result of computing the distribution function opacities. They existed only for scaled solar abundances and each abundance required 100 Cray hours to compute. In order to make opacity sampling viable I had to find a way to determine the Rosseland opacity using no computer time. Michele Gerbaldi finally forced me to solve the problem in May 1995.

2. Virtual Rosseland opacity

All versions of the ATLAS model atmosphere program compute the Rosseland opacity for the temperature and pressure of each layer of the model for each iteration. ATLAS12 now saves all these values as it iterates. It finds the Rosseland opacity for convection and the temperature correction by guessing

from the nearest saved values. The procedure is to divide the T,P plane into quadrants around the point of interest, then to pick out the nearest tabulated point in each quadrant, and then to linearly interpolate among those points. Often not all the quadrants are occupied so various ad hoc guesses are made. Since these Rosseland opacities are computed for the abundances actually used in the model they can be more accurate, even when guessed, than pretabulated values. The models now converge well.
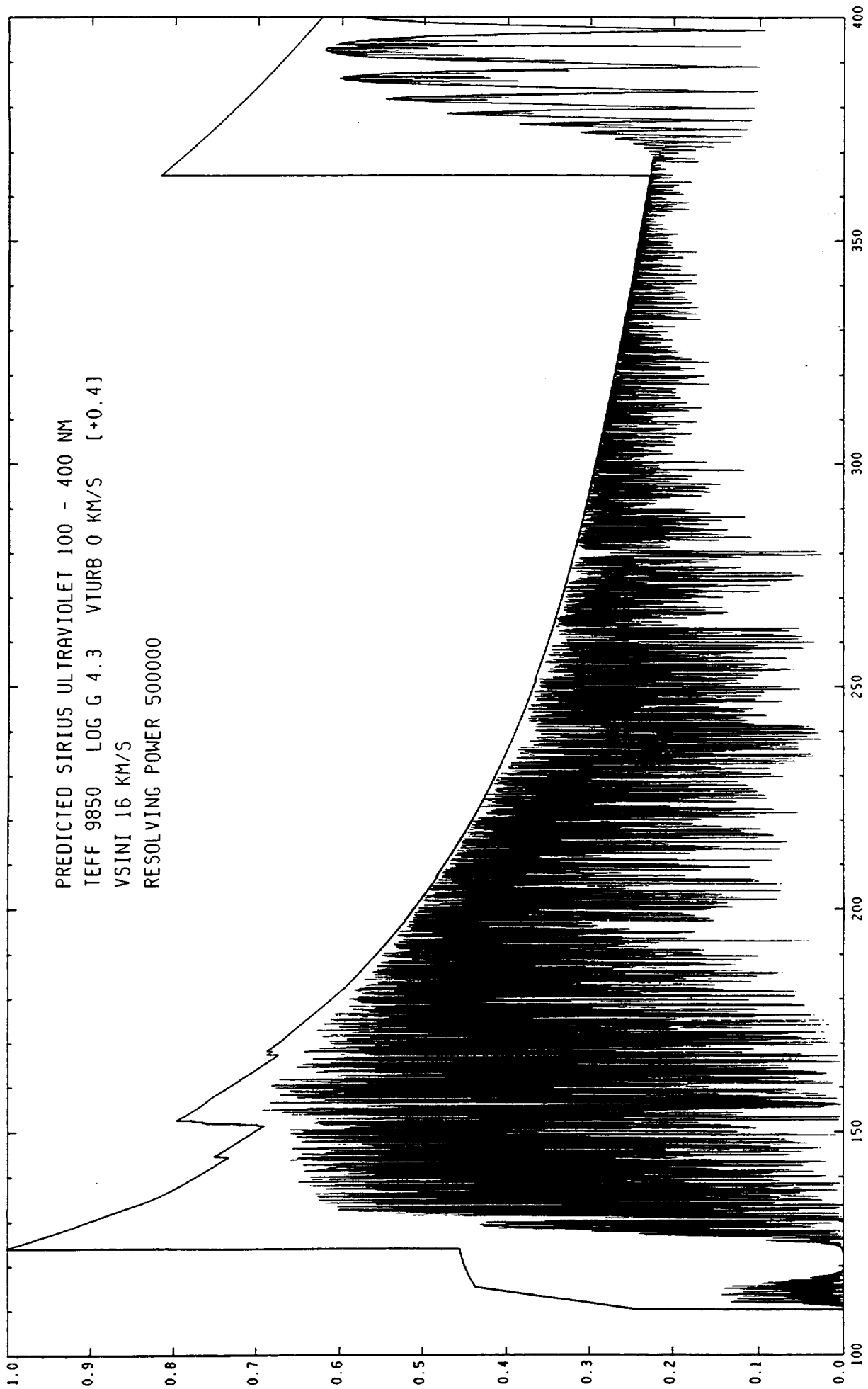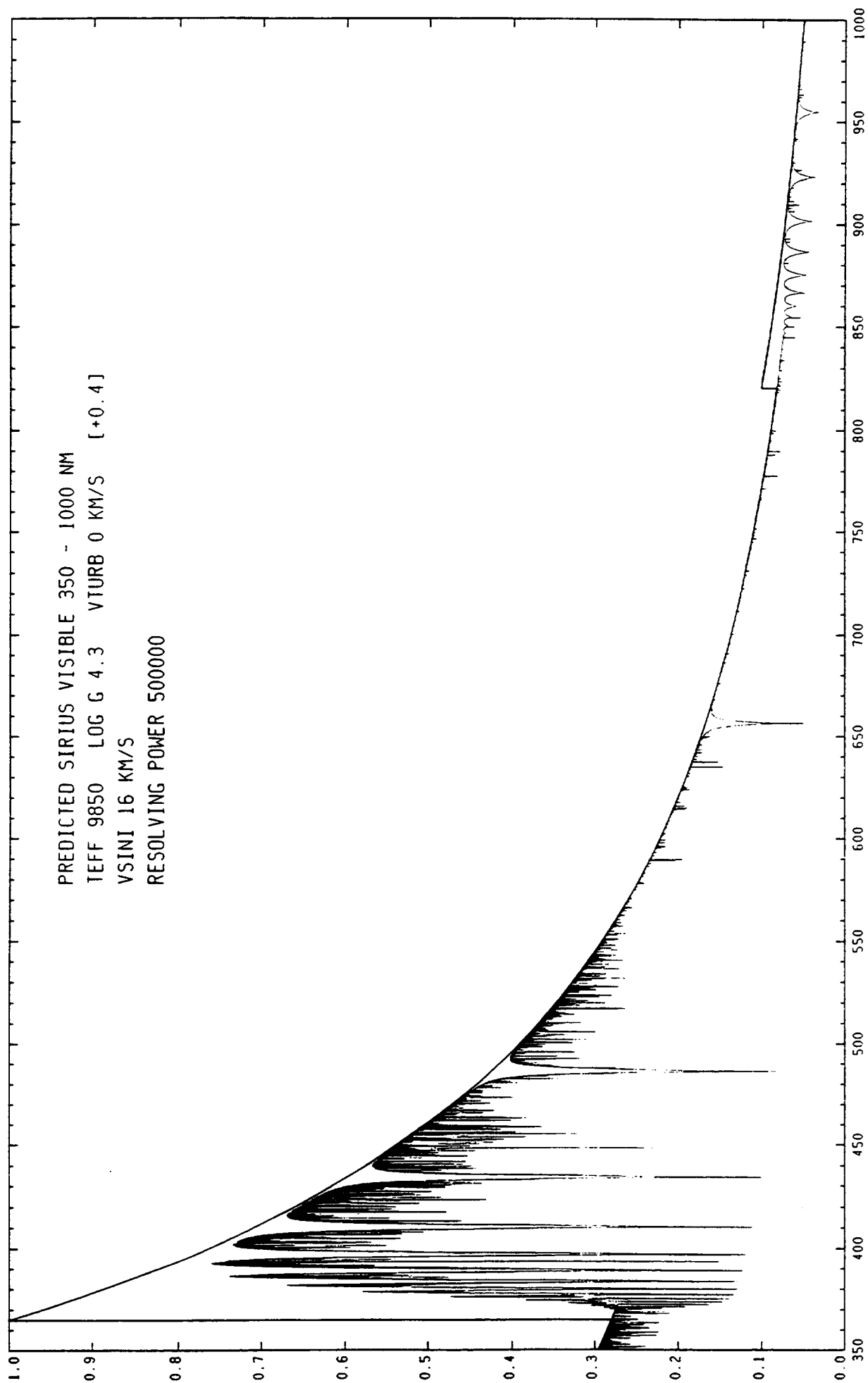
3. Computing the whole spectrum

When actually working with ATLAS12 sampled fluxes, Castelli and I found that, while quite accurate for predicting the total flux, the fluxes are not accurate in intermediate or narrow bandpass intervals because the sample size is too small. I wrote a special stripped version of the spectrum synthesis program SYNTHE to generate the surface flux for the converged model using the line data from CD-ROMs 1 and 15. Plots showing sample calculations of complete spectra are given in Kurucz (1994) and Kurucz (1995). Figures 1, 2, and 3 show the first three microns of the Sirius spectrum. As most of the line positions are predicted, the computed flux spectrum is not realistic when compared to a high resolution observed spectrum. It is possible to select only the subset of lines with accurate wavelengths, but many lines will be missing. This difficulty can be removed only by improving laboratory spectrum analyses. When more energy levels are known, more line positions can be computed accurately.
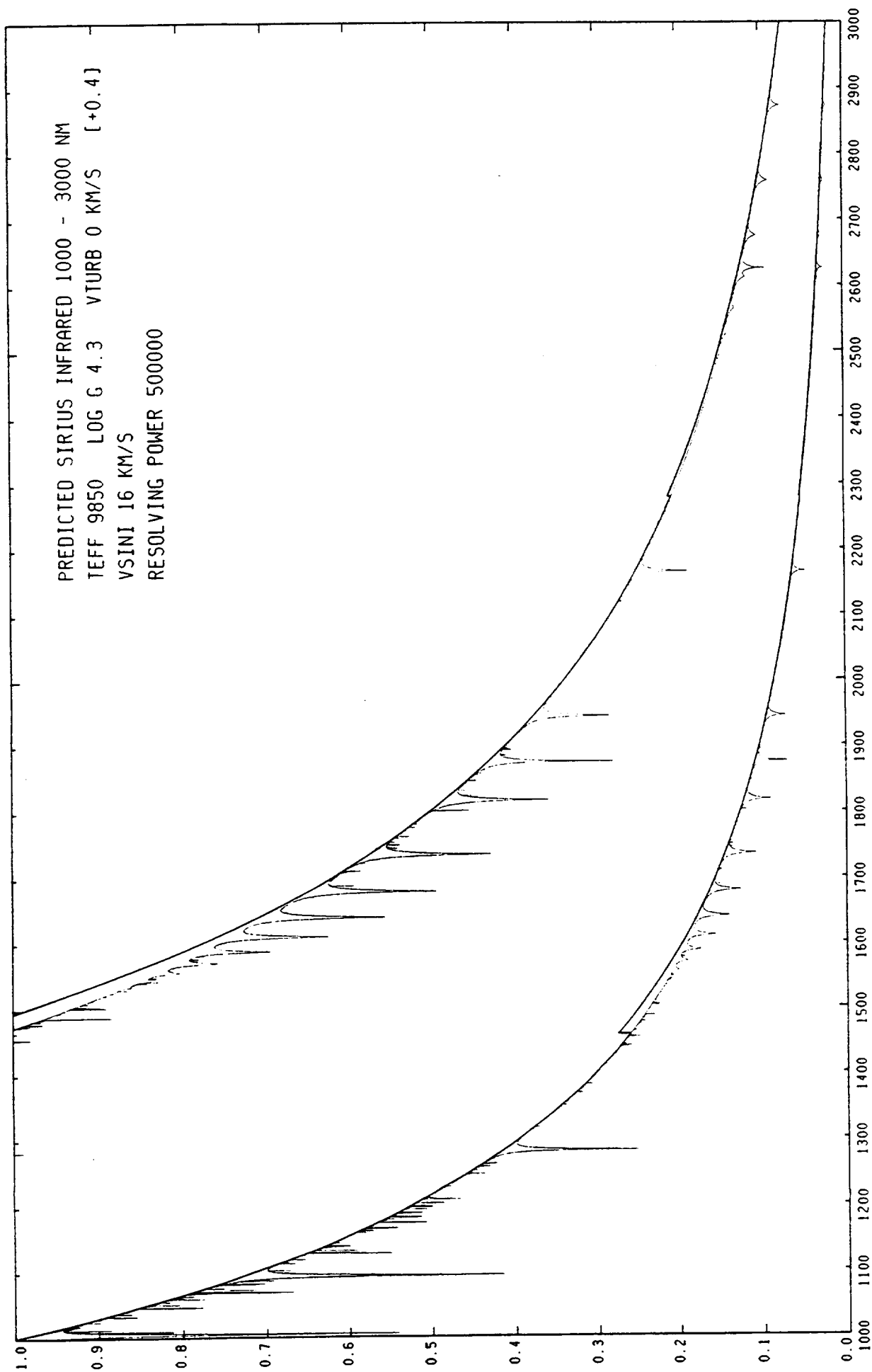
The spectrum is computed in pieces typically at resolving power 500000. It is actually computed as 17 intensity spectra spread across the disk of the star from center to limb. These pieces are merged into 17 continuous intensity spectra. Then rotationally broadened flux spectra are computed for a number of values of v sin i, still at a resolving power of 500000, by interpolating and integrating over the disk. Alternatively, the pieces can be rotationally broadened and then merged. In these calculations all information about individual lines is thrown away. To get the complete information the calculation must be made with the full SYNTHE program. These high resolution spectra can be used directly or can be instrumentally broadened to compare to low resolution observations. The intensity spectra from different models can be combined to mimic surface features.

4. Computing Rosseland and distribution function opacities

If one takes the fast spectrum synthesis program just described and removes everything about computing the radiation field, one is left with all the physics needed to compute opacities. Instead of using a real model as input one uses a table of temperatures and pressures or temperatures and densities. All that remains is to program the bookkeeping operations. The line opacity spectrum or the total opacity spectrum can be statistically analyzed to tabulate line- or total distribution functions, or the total opacity spectrum can be directly inserted into the Rosseland integrand. I am debugging these programs now.

PREDICTED SIRIUS ULTRAVIOLET 100 - 400 NM

TEFF 9850   LOG G 4.3   VTURB 0 KM/S   [+0.4]

VSINI 16 KM/S

RESOLVING POWER 500000

PREDICTED SIRIUS VISIBLE 350 - 1000 NM

TEFF 9850   LOG G 4.3   VTURB 0 KM/S   [+0.4]

VSINI 16 KM/S

RESOLVING POWER 500000

PREDICTED SIRIUS INFRARED 1000 - 3000 NM

TEFF 9850   LOG G 4.3   VTURB 0 KM/S   [+0.4]

VSINI 16 KM/S

RESOLVING POWER 500000

5. Distribution

I will distribute a CD-ROM with programs ATLAS12, the fast SYNTHE, a new distribution function program, and a new Rosseland opacity program. These programs all read line data from CD-ROMs 1 and 15. All the CD-ROMs cited in this paper can be requested from the author at the email address listed above.

References

Castelli, F. and Kurucz, R. L. 1994. A&A 281, 817

Kurucz, R. L. 1993. in *Peculiar versus Normal Phenomena in A-type and Related Stars*, M. M. Dworetsky, F. Castelli, and R. Faraggiana, eds., A.S.P. Conference Series, 87

Kurucz, R. L. 1994, in *Molecules in the Stellar Environment*, U. G. Jørgensen, ed., Springer-Verlag, Berlin, 282

Kurucz, R. L. 1995. in *Highlights of Astronomy*, Vol. 10, I. Appenzeller, ed., 407